THE JOURNAL OF BIOLOGICAL CHEMISTRY VOL. 291, NO. 12, pp. 6218–6231, March 18, 2016

The Ankrd13 Family of Ubiquitin-interacting Motif-bearing Proteins Regulates Valosin-containing Protein/p97 Protein-mediated Lysosomal Trafficking of Caveolin 1*

Received for publication, December 14, 2015, and in revised form, January 15, 2016 Published, JBC Papers in Press, January 21, 2016, DOI 10.1074/jbc.M115.710707

Daocharad Burana[‡], Hidehito Yoshihara[§], Hidetaka Tanno[‡], Akitsugu Yamamoto[¶], Yasushi Saeki[§], Keiji Tanaka[§], and Masayuki Komada[‡1]

From the [‡]Department of Biological Sciences, Tokyo Institute of Technology, Yokohama 226-8501, Japan, the [§]Laboratory of Protein Metabolism, Tokyo Metropolitan Institute of Medical Science, Setagaya, Tokyo 156-8506, Japan, and the [¶]Department of Bioscience, Nagahama Institute of Bioscience and Technology, Nagahama 526-0829, Japan

Caveolin 1 (Cav-1) is an oligomeric protein that forms flask-shaped, lipid-rich pits, termed caveolae, on the plasma membrane. Cav-1 is targeted for lysosomal degradation in ubiquitination- and valosin-containing protein (VCP)-dependent manners. VCP, an ATPase associated with diverse cellular activities that remodels or segregates ubiquitinated protein complexes, has been proposed to disassemble Cav-1 oligomers on the endosomal membrane, facilitating the trafficking of Cav-1 to the lysosome. Genetic mutations in VCP compromise the lysosomal trafficking of Cav-1, leading to a disease called inclusion body myopathy with Paget disease of bone and/or frontotemporal dementia (IBMPFD). Here we identified the Ankrd13 family of ubiquitin-interacting motif (UIM)-containing proteins as novel VCP-interacting molecules on the endosome. Ankrd13 proteins formed a ternary complex with VCP and Cav-1 and exhibited high binding affinity for ubiquitinated Cav-1 oligomers in an UIM-dependent manner. Mass spectrometric analyses revealed that Cav-1 undergoes Lys-63-linked polyubiquitination, which serves as a lysosomal trafficking signal, and that the UIMs of Ankrd13 proteins bind preferentially to this ubiquitin chain type. The overexpression of Ankrd13 caused enlarged hollow late endosomes, which was reminiscent of the phenotype of the *VCP* mutations in IBMPFD. Overexpression of Ankrd13 proteins also stabilized ubiquitinated Cav-1 oligomers on the limiting membrane of enlarged endosomes. The interaction with Ankrd13 was abrogated in IMBPFD-associated VCP mutants. Collectively, our results suggest that Ankrd13 proteins cooperate with VCP to regulate the lysosomal trafficking of ubiquitinated Cav-1.

Caveolae are flask-shaped pits in the lipid-rich domains of the plasma membrane. They are structured by an electron-dense, membrane-spanning oligomeric protein called caveolin (Cav)[2] and have been implicated in various cellular activities, including endocytosis and signal transduction (1). The mammalian Cav family consists of three members: Cav-1, Cav-2, and Cav-3. Caveolae mainly comprise either Cav-1 or Cav-3 homo-oligomers, which, at lower proportions, form hetero-oligomers with Cav-2 (2). Cav-1 and Cav-2 are expressed ubiquitously, whereas Cav-3 is primarily expressed in striated muscle. Cav proteins associate with the plasma membrane through their central regions, leaving the N- and C-terminal regions oriented toward the cytoplasm (3). Newly synthesized Cav monomers, after their insertion into the endoplasmic reticulum membrane, are transported to the Golgi apparatus, where they are oligomerized into SDS-resistant 8S oligomers together with cholesterol. The 8S oligomers are finally transported to the plasma membrane, where they form 70S oligomers and are stabilized by regulatory proteins, such as cavin, to constitute complete caveolae (2, 4).

Cav-1 undergoes endocytosis from the plasma membrane and is transported to the lysosome for degradation in a ubiquitination-dependent manner (5). Ubiquitination is a post-translational modification of proteins with a 76-amino acid protein called ubiquitin (Ub). Ub is conjugated either directly to the Lys residues of various intracellular proteins or through another Ub moiety to form Ub chains (6). All the seven Lys residues of Ub are capable of forming Ub chains. Among the different types of polyubiquitination, Lys-48-linked and Lys-63-linked types are the most abundant in the cell (7, 8). Lys-48-linked polyubiquitination is known for its role in proteasomal degradation of intracellular proteins (6). On the other hand, Lys-63-linked polyubiquitination serves as a tag that targets plasma membrane proteins to the lysosome for degradation via the early endosome and late endosome/multivesicular body (MVB) (9, 10). The Ub moieties of plasma membrane proteins are recognized sequentially on the early endosome by three Ub-binding protein complexes called the endosomal sorting complex required for transport (ESCRT) 0, I, and II, and this is

* This work was supported by Ministry of Education, Culture, Sports, Science, and Technology of Japan Grants-in-Aid 24112003 (to M. K.), 24112008 (to Y. S.), and 21000012 (to K. T.). The authors declare that they have no conflicts of interest with the contents of this article.

[1] To whom correspondence should be addressed: Dept. of Biological Sciences, Tokyo Institute of Technology, 4259-B16 Nagatsuta, Midori, Yokohama 226-8501, Japan. Tel.: 81-45-924-5703; Fax: 81-45-924-5771; E-mail: makomada@bio.titech.ac.jp.

[2] The abbreviations used are: Cav, caveolin; Ub, ubiquitin; MVB, multivesicular body; ESCRT, endosomal sorting complex required for transport; VCP, valosin-containing protein; UIM, ubiquitin-interacting motif; NEM, *N*-ethylmaleimide; UBXD, ubiquitin regulatory X domain-containing protein; UBX, ubiquitin regulatory X; CI-M6PR, cation-independent mannose 6-phospate receptor; IBMPFD, inclusion body myopathy with Paget disease of bone and/or frontotemporal dementia.

followed by the ESCRT-III-mediated incorporation of the ubiquitinated cargo into the inner vesicles of the MVB (11). Although the lysosomal trafficking of Cav-1 depends on its ubiquitination and the ESCRT machinery (5), valosin-containing protein (VCP)/p97 is also shown to be required (12). VCP is a homohexameric ATPase associated with diverse cellular activities that utilizes energy from ATP hydrolysis to remodel or segregate ubiquitinated protein complexes (13, 14). It plays important roles in a myriad of cellular activities, including endoplasmic reticulum-associated degradation, in which VCP pulls misfolded, newly synthesized proteins out of the endoplasmic reticulum membrane into the cytoplasm for proteasomal degradation (15). Mutations in the *VCP* gene have been linked to various neurodegenerative diseases associated with impaired clearance of protein aggregates, including inclusion body myopathy with Paget disease of bone and/or frontotemporal dementia (IBMPFD), amyotrophic lateral sclerosis, and Parkinson disease (16, 17). The WT, but not disease mutants, of VCP binds to Cav-1, and the expression of the VCP mutants causes the accumulation of Cav-1 to aberrantly enlarged late endosomes, suggesting that dysfunction of VCP-mediated Cav-1 trafficking is causative of neurodegenerative diseases (12).

The ankyrin repeat domain (Ankrd) 13 family of proteins, including Ankrd13A, 13B, and 13D, consists of proteins with three ankyrin repeat domains in the N-terminal region and three or four Ub-interacting motifs (UIMs) in the C-terminal region. We have reported previously that Ankrd13 proteins bind via UIMs to ligand-activated, ubiquitinated EGF receptors on the plasma membrane, regulating its rapid endocytosis from the cell surface (18). However, Ankrd13 proteins are mainly localized on endosomes (18), raising the possibility that they have an unidentified endosomal function. In this study, we demonstrated this novel role for Ankrd13 proteins on the endosome.

Experimental Procedures

cDNA Expression Constructs—FLAG-tagged Ankrd13 expression vectors were constructed using the mammalian expression vector pME (19) as described previously (18). Human VCP and Cav-1 cDNAs were purchased from GE Healthcare/Dharmacon, tagged C-terminally with the FLAG (VCP and Cav-1) or HA (Cav-1) epitope, and inserted into pME. The FLAG-tagged rat ubiquitin regulatory X domain-containing protein (UBXD) 1 expression vector was provided by M. Nagahama (Meiji Pharmaceutical University) (20). The FLAG-STAM1 expression vector was constructed as described previously (21). The QuikChange site-directed mutagenesis system (Stratagene, La Jolla, CA) was used to introduce point mutations into the VCP and Cav-1 cDNAs.

Cell Culture and DNA Transfection—HeLa and COS-7 cells were grown in DMEM supplemented with 10% FBS. DNAs were transfected into cells with jetPRIME transfection reagent (Polyplus-transfection, Illkirch, France) for 24 h, FuGENE6 transfection reagent (Roche Diagnostics) for 48 h, or linear polyethylenimine (molecular mass, 25 kDa; 3 μg/ml, Wako Pure Chemicals, Osaka, Japan) for 48 h. For EGF treatment, cells were cultured in DMEM supplemented with 0.5% FBS for 24 h and subsequently incubated with human EGF (100 ng/ml; PeproTech, Rocky Hill, NJ) at 37 °C.

Preparation of Cell Lysates—Cells were solubilized in 20 mM Tris-HCl (pH 7.4), 100 mM NaCl, 50 mM NaF, 0.5% Nonidet P-40, 1 mM EDTA, 10 mM *N*-ethylmaleimide (NEM) (unless indicated), 1 mM PMSF, 1 μg/ml aprotinin, 1 μg/ml leupeptin, and 1 μg/ml pepstatin A. After solubilization at 4 °C for 30 min, cell lysates were cleared by centrifugation at 12,000 × *g* for 15 min. To examine Cav-1 oligomer levels, cells were solubilized in extraction buffer (25 mM Tris-HCl (pH 7.4), 150 mM KCl, 5 mM $MgCl_2$, 1% Triton X-100, 5% glycerol, 2 mM β-mercaptoethanol, 10 mM NEM, 1 mM PMSF, 1 μg/ml aprotinin, 1 μg/ml leupeptin, and 1 μg/ml pepstatin A) (12). To prepare lysates with the hot lysis method, cells were solubilized in 20 mM Tris-HCl (pH 7.4), 150 mM NaCl, 1% SDS, and 1 mM EDTA for 12 min at 100 °C. After centrifugation, the supernatants were diluted 4-fold with 1.33% Triton X-100. Protein concentrations were determined with the BCA assay kit (Thermo Scientific, Rockford, IL).

To determine Ankrd13A-associated Ub chains by MS, cells were solubilized in 1% Triton X-100 lysis buffer (20 mM Tris-HCl (pH 7.4), 100 mM NaCl, 1% Triton X-100, 1 mM EDTA, 10 mM iodoacetic acid, 40 μM bortezomib (LC Laboratories, Woburn, MA), 50 μM PR619 (Abcam, Cambridge, UK), PhosSTOP phosphatase inhibitor mixtures (Roche Diagnostics), and cOmplete EDTA-free protease inhibitor mixture (Roche Diagnostics)). To access the Ub modifications of Cav-1, cells were lysed in radio-immunoprecipitation assay buffer (50 mM Tris-HCl (pH 8.0), 150 mM NaCl, 1% SDS, 0.5% deoxycholate, 10% glycerol, 10 mM iodoacetic acid, 40 μM bortezomib, 50 μM PR619, PhosSTOP phosphatase inhibitor mixtures, and cOmplete EDTA-free protease inhibitor mixture). Cell lysates were collected, stored in Protein LoBind tubes (Eppendorf, Hamburg, Germany), and sonicated on ice at 30-s intervals with a 1-s short burst and 1-s rest at a moderate power (UR21P, Tomy Seiko, Tokyo, Japan). After centrifugation at 12,000 × *g* for 10 min twice, the supernatants were collected into new Protein LoBind tubes and subjected to immunoprecipitation. For the cell lysates in radioimmune precipitation assay buffer, supernatants were diluted 10-fold in 1% Triton X-100 lysis buffer prior to immunoprecipitation. Protein concentrations were determined using protein assay dye reagent concentrate (Bio-Rad).

Immunoprecipitation and Immunoblotting—Immunoprecipitation was performed using standard procedures. Anti-FLAG (1 μg, clone M2, Sigma-Aldrich, St. Louis, MO), anti-HA (1.25 μg, clone 12CA5, Roche Diagnostics), anti-VCP (1 μg, catalog no. ab11433, Abcam), and anti-EGF receptor (1 μg, clone 6F1, MBL, Nagoya, Japan) antibodies were used for immunoprecipitation. The indicated amounts of antibodies were used for ~0.5 mg of total proteins in 250 μl of the cell lysate. To immunoprecipitate the Flag-VCP·HA-Cav-1·Ankrd13A ternary complex, cell lysates were precleared in protein A-Sepharose beads (GE Healthcare) in the absence of an antibody at 4 °C for 1 h, and FLAG-VCP was immunoprecipitated with anti-FLAG antibody-conjugated beads (M2 affinity gel, Sigma-Aldrich). Bound FLAG-VCP was eluted from the beads with the FLAG peptide (200 μg/ml, Sigma-Aldrich) and subjected to a standard second immunoprecipita-

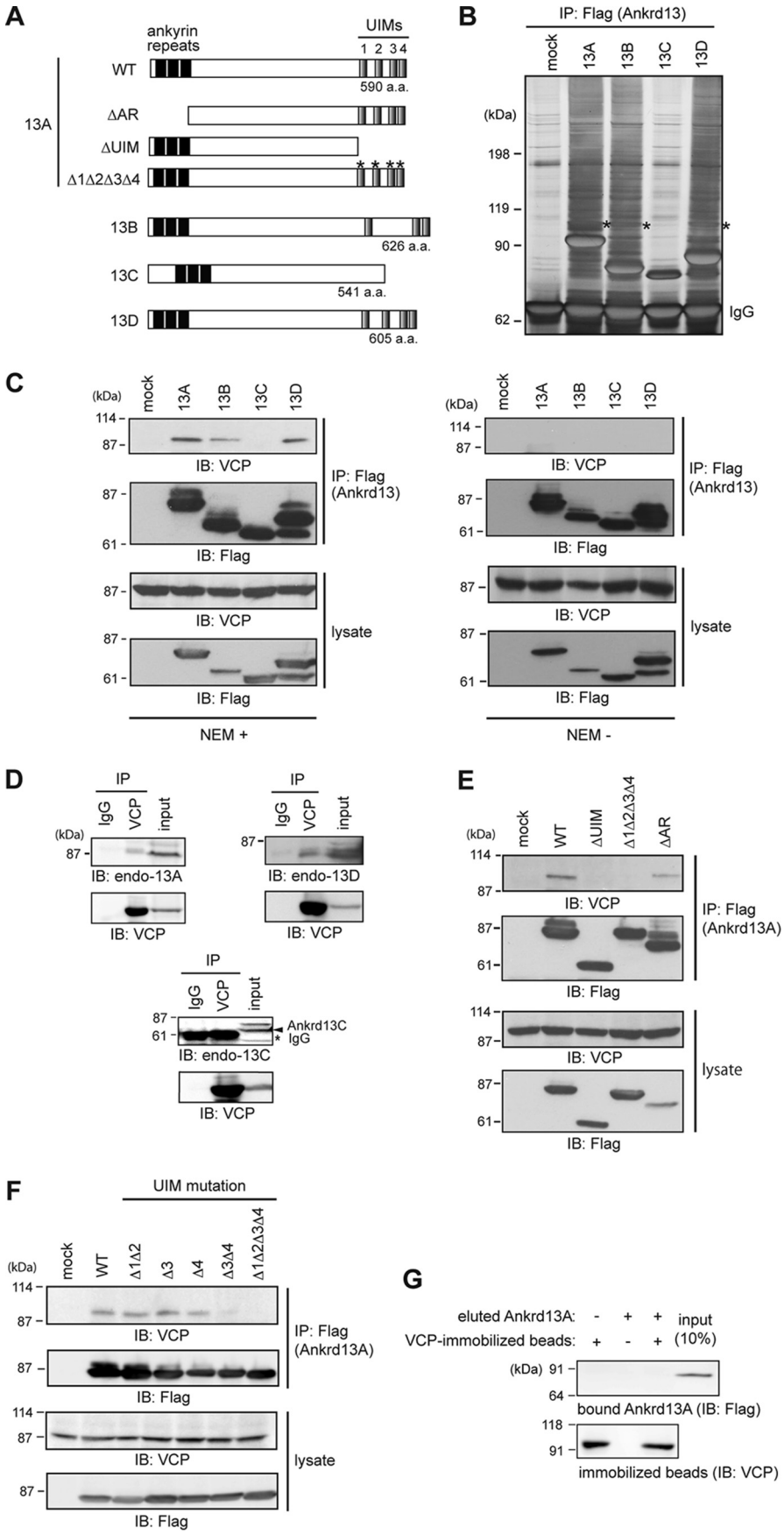
A
ankyrin repeats
UIMs
1 2 3 4
WT
590 a.a.
13A
ΔAR
ΔUIM
Δ1Δ2Δ3Δ4
13B
626 a.a.
13C
541 a.a.
13D
605 a.a.
B
IP: Flag (Ankrd13)
mock
13A
13B
13C
13D
(kDa)
198
119
90
62
IgG
C
IB: VCP
IP: Flag (Ankrd13)
IB: Flag
lysate
NEM +
NEM -
D
IP
IgG
VCP
input
IB: endo-13A
IB: endo-13D
IB: endo-13C
Ankrd13C
IgG
E
mock
WT
ΔUIM
Δ1Δ2Δ3Δ4
ΔAR
IP: Flag (Ankrd13A)
F
UIM mutation
mock
WT
Δ1Δ2
Δ3
Δ4
Δ3Δ4
Δ1Δ2Δ3Δ4
G
eluted Ankrd13A:
VCP-immobilized beads:
input (10%)
bound Ankrd13A (IB: Flag)
immobilized beads (IB: VCP)

tion. Primary antibodies for immunoblotting were as follows: anti-EGF receptor (1 μg/ml, clone 6F1, MBL), anti-Ub (1 μg/ml, clone FK2, MBL), anti-Ub (0.76 μg/ml, catalog no. Z0458, Dako, Glostrup, Denmark), mouse anti-FLAG (1 μg/ml, clone M2, Sigma-Aldrich), rabbit anti-FLAG (1 μg/ml, catalog no. 7425, Sigma-Aldrich), anti-α-tubulin (0.02 μg/ml, catalog no. ab15246, Abcam), anti-HA (0.1 μg/ml, clone 3F10, Roche Diagnostics), anti-VCP (0.25 μg/ml, clone 18/VCP, BD Transduction Laboratories), anti-Ankrd13A (2 μg/ml, catalog no. HPA039488, Atlas Antibodies, Stockholm, Sweden), anti-Ankrd13B (2 μg/ml, catalog no. HPA051886, Atlas Antibodies), anti-Ankrd13B (1:800) (18), anti-Ankrd13C (1:800) (18), and anti-Ankrd13D (1:800) (18) antibodies. Secondary antibodies were peroxidase-conjugated anti-mouse, -rat, and -rabbit IgG antibodies (GE Healthcare). An anti-FLAG (clone M2) peroxidase conjugate (1 μg/ml, Sigma-Aldrich) was also used. Blots were detected using ECL and ECL Prime Western blotting detection reagents (GE Healthcare). The intensity of bands in immunoblotted membranes was quantified using ImageJ (National Institutes of Health, Bethesda, MD).

Immunofluorescence Staining—Cells were fixed in 4% paraformaldehyde in PBS, permeabilized in 0.2% Triton X-100 in PBS, and blocked in 5% FBS in PBS. Cells were then incubated with rabbit anti-FLAG (2 μg/ml, catalog no. 7425, Sigma-Aldrich), mouse anti-FLAG (2 μg/ml, clone M2, Sigma-Aldrich), anti-HA (1 μg/ml, clone 3F10, Roche Diagnostics), anti-VCP (1:500, catalog no. ab11433, Abcam), anti-EEA1 (1 μg/ml, BD Transduction Laboratories), anti-CI-M6PR (5 μg/ml, provided by E. Kominami, Juntendo University, Tokyo, Japan), and anti-Ub (10 μg/ml, clone FK2, MBL) antibodies. Secondary antibodies were Alexa Fluor 488- and 594-conjugated anti-mouse, -rat, and -rabbit IgG antibodies (1:1000, Invitrogen). Fluorescence images were captured with a laser-scanning confocal microscope (LSM780, Carl Zeiss, Oberkochen, Germany).

MALDI-TOF MS—To identify novel Ankrd13-interacting proteins, immunoprecipitated Ankrd13 proteins were subjected to SDS-PAGE, and the gel was stained using a silver stain MS kit (Wako Pure Chemical). Protein bands of interest were excised, diced into small pieces, destained, chemically reduced, and alkylated according to standard procedures. Gels were trypsinized overnight at 37 °C with Trypsin Gold-MS grade (10 ng/μl, Promega, Madison, WI) in 25 mM ammonium bicarbonate. Digests were quenched and extracted by treatment with 25% acetonitrile/0.5% TFA and sonication. The extracted peptides were collected and concentrated by speed-vac. MALDI-TOF MS analysis was carried out using Ultraflex P TOF/TOF (Bruker Daltonics, Billerica, MA). Raw data were processed and analyzed using flexControl and flexAnalysis software (Bruker Daltonics), respectively. Biotools software (Bruker Daltonics) was used to analyze MS spectra and match the peptide sequences with the MASCOT database (Matrix Science, Boston, MA).

LC-MS/MS—LC-MS/MS using the absolute quantification strategy was performed as described previously (22). Briefly, to determine Ankrd13A-associated Ub chains as well as the Ub modification of Cav-1, immunoprecipitated Ankrd13A and Cav-1 were subjected to SDS-PAGE using NuPAGE BisTris gels (Life Technologies). Gels were stained with bio-safe Coomassie (Bio-Rad) and washed extensively with ultrapure water. The protein-loaded regions of the gels were excised, diced into 1-mm^3 cubes, destained, and trypsinized overnight at 37 °C with modified sequencing-grade trypsin (20 ng/μl, Promega). Digests were quenched, extracted, and recovered into fresh Protein LoBind tubes. The extracted peptides were concentrated to 15 μl using speed-vac.

Seven microliters of the concentrated peptide solution were mixed with 13 μl of 40 fmol of the Ub absolute quantification peptides (22), 0.1% TFA, and 0.05% H_2O_2, and an aliquot of the solution containing 10 fmol of the Ub peptide was analyzed on a nanoflow ultra high performance LC instrument (Easy nLC 1000, Q-Exactive MS, and nanoelectrospray ion source (Thermo Fisher Scientific)). Raw data were processed by Xcalibur (Thermo Fisher Scientific). MS spectra were analyzed using PinPoint software version 1.3 (Thermo Fisher Scientific).

Results

Ankrd13 Proteins Interact with VCP—To determine the possible endosomal function of Ankrd13 proteins, we attempted to identify their novel binding partners using co-immunoprecipitation experiments. FLAG-tagged Ankrd13A, 13B, 13C, and 13D proteins (Fig. 1*A*) were expressed individually in HeLa cells and immunoprecipitated from cell lysates with the anti-FLAG antibody in the presence of NEM. Silver staining of the precipitated proteins after SDS-PAGE revealed that an ~100-kDa protein co-precipitates with UIM-bearing Ankrd13A, 13B, and 13D but not with 13C lacking the UIMs (Fig. 1*B*, *asterisks*). The protein band was excised from the gel, trypsinized, and analyzed by MALDI-TOF MS, leading to identification of the protein as VCP/p97/Cdc48 (Mascot score, 157; data not shown).

The interaction was confirmed by anti-VCP immunoblotting, which detected VCP in the anti-FLAG immunoprecipitates from FLAG-Ankrd13A-, 13B-, and 13D-transfected cell lysates only in the presence of NEM (Fig. 1*C*). Because NEM inhibits cysteine protease-type deubiquitinases, these results

FIGURE 1. **Ankrd13 proteins interact with VCP.** *A*, schematics of the Ankrd13A-13D and Ankrd13A mutants used routinely in this study. *a.a.*, amino acids. *B*, HeLa cells were transfected with FLAG-tagged Ankrd13 proteins and lysed in the presence of NEM. Ankrd13 proteins were immunoprecipitated (*IP*) with an anti-FLAG antibody, and the precipitated proteins were detected by silver staining after SDS-PAGE. *Asterisks*, the band corresponding to VCP; *IgG*, IgG heavy chain used for immunoprecipitation. *C*, HeLa cells transfected with FLAG-tagged Ankrd13 proteins were lysed in the presence (*left panel*) or absence (*right panel*) of NEM. Lysates were immunoprecipitated with an anti-FLAG antibody and immunoblotted (*IB*) with the indicated antibodies. Cell lysates were also immunoblotted with the indicated antibodies. *D*, the lysate of untransfected HeLa cells, prepared in the presence of NEM, was immunoprecipitated with an anti-VCP antibody and immunoblotted with antibodies to Ankrd13A, 13C, or 13D. *E* and *F*, HeLa cells transfected with the indicated FLAG-Ankrd13A mutants were lysed in the presence of NEM, immunoprecipitated with an anti-FLAG antibody, and immunoblotted with the indicated antibodies. *G*, COS-7 cells were transfected with FLAG-Ankrd13A and lysed using the hot lysis method. FLAG-Ankrd13A was immunoprecipitated with an anti-FLAG antibody and eluted with the FLAG peptide. VCP was immunopurified similarly from the hot lysis lysate of untransfected COS-7 cells and immobilized on anti-VCP antibody-coupled beads. Eluted FLAG-Ankrd13A was incubated with VCP-immobilized beads, and bound Ankrd13A was examined by anti-FLAG immunoblotting. All experiments were performed at least three times.

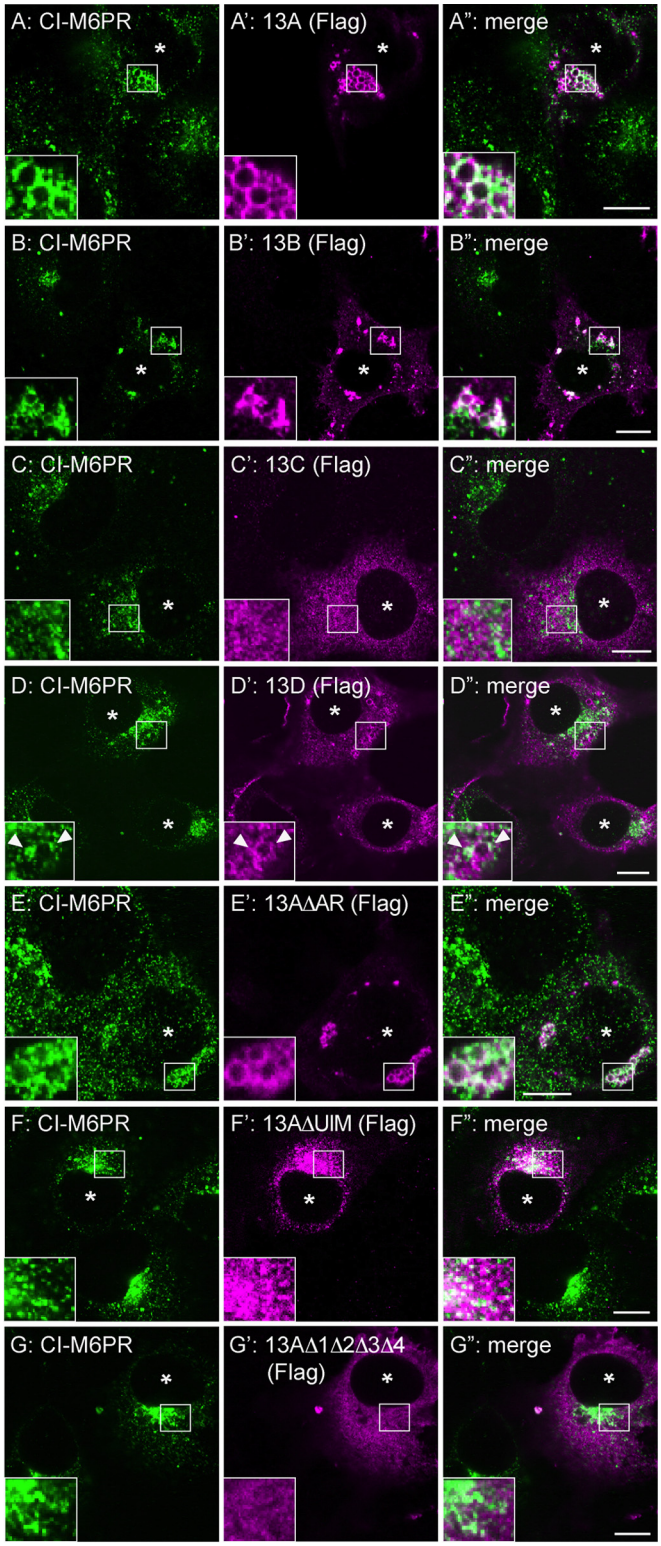

FIGURE 2. **Ankrd13 overexpression causes enlarged late endosomes.** COS-7 cells were transfected with FLAG-tagged Ankrd13 proteins or Ankrd13A mutants and double-stained with anti-CI-M6PR (*A–G*) and anti-FLAG (*A′–G′*) antibodies. The *arrowheads* in *D–D″* indicate the co-localization sites of Ankrd13D with CI-M6PR. *Asterisks* indicate nuclei in FLAG-Ankrd13-expressing cells. *Insets* show higher magnification images of regions indicated by *squares*. *Scale bars* = 10 μm. All panels are representatives of four independent experiments.

suggest that the Ankrd13-VCP interaction requires protein ubiquitination. The binding of endogenous Ankrd13 proteins to VCP was then examined. Untransfected HeLa cells were lysed in the presence of NEM and immunoprecipitated with the control IgG or anti-VCP antibody. Blotting of the precipitates with specific antibodies for Ankrd13A, 13C, and 13D showed that endogenous Ankrd13A and 13D, but not 13C, were co-precipitated successfully with endogenous VCP (Fig. 1*D*). The expression of endogenous Ankrd13B was not detected in HeLa cells with our or commercially available anti-Ankrd13B antibodies (data not shown).

Interaction of Ankrd13A with VCP Is UIM-dependent and Indirect—To identify the region in Ankrd13 proteins required for VCP binding, HeLa cells were transfected with FLAG-tagged Ankrd13A mutants lacking ankyrin repeats (ΔAR), lacking the UIM region (ΔUIM), or harboring Δ1Δ2Δ3Δ4 point mutations with substitutions in the invariant Ala/Val and Ser residues in the four UIMs (Fig. 1*A*) (18). Cell lysates were subjected to immunoprecipitation with the anti-FLAG antibody, and co-precipitated VCP was detected by immunoblotting. ΔAR bound to VCP, whereas ΔUIM and Δ1Δ2Δ3Δ4 did not (Fig. 1*E*). We further examined the VCP binding of Ankrd13A mutants with point mutations in individual UIMs. Consistent with our previous findings that the two C-terminally located UIMs (UIM3 and UIM4) are important for Ub binding (18), the VCP-binding ability was reduced in the mutant with mutations in UIM3 and UIM4 (Fig. 1*F*, *Δ3Δ4*). VCP binding of the mutant with mutations in UIM1 and UIM2 (Δ1Δ2) and that in mutants with mutations individually in UIM3 (Δ3) or UIM4 (Δ4) was not affected significantly (Fig. 1*F*), suggesting that Ub-binding ability is required for Ankrd13 proteins to interact with VCP.

We subsequently examined whether the Ankrd13-VCP interaction is direct. FLAG-Ankrd13A was expressed in COS-7 cells, and the cells were lysed at 100 °C in the presence of 1% SDS to dissociate non-covalently associated proteins from Ankrd13A. Ankrd13A was renatured, immunoprecipitated from the cell lysate using the anti-FLAG antibody, and eluted from the antibody with the FLAG peptide. VCP was also immunoprecipitated with the anti-VCP antibody from the lysate of untransfected COS-7 cells prepared in the presence of 1% SDS at 100 °C. VCP-immobilized beads were incubated with eluted FLAG-Ankrd13A, and, after washing the beads, the precipitates were blotted with anti-FLAG antibody. FLAG-Ankrd13A was not pulled down with VCP (Fig. 1*G*). To exclude the possibility that proteins were not functionally renatured after boiling in SDS, we performed control experiments with known direct binding partners for Ankrd13A (*i.e.* ubiquitinated EGF receptor) (18) and VCP (*i.e.* co-factor UBXD1) (20). As expected (18), the eluted FLAG-Ankrd13A was pulled down with EGF receptor immunopurified from the lysate of EGF-treated cells prepared in boiling 1% SDS (data not shown). A direct interaction between VCP and UBXD1 was also confirmed in an experiment in which FLAG-UBXD1 was immunopurified from cell lysates prepared in 1% SDS at 100 °C and pulled down with VCP-immobilized beads (data not shown). Collectively, these results suggest that the interaction between Ankrd13A and VCP is indirect.

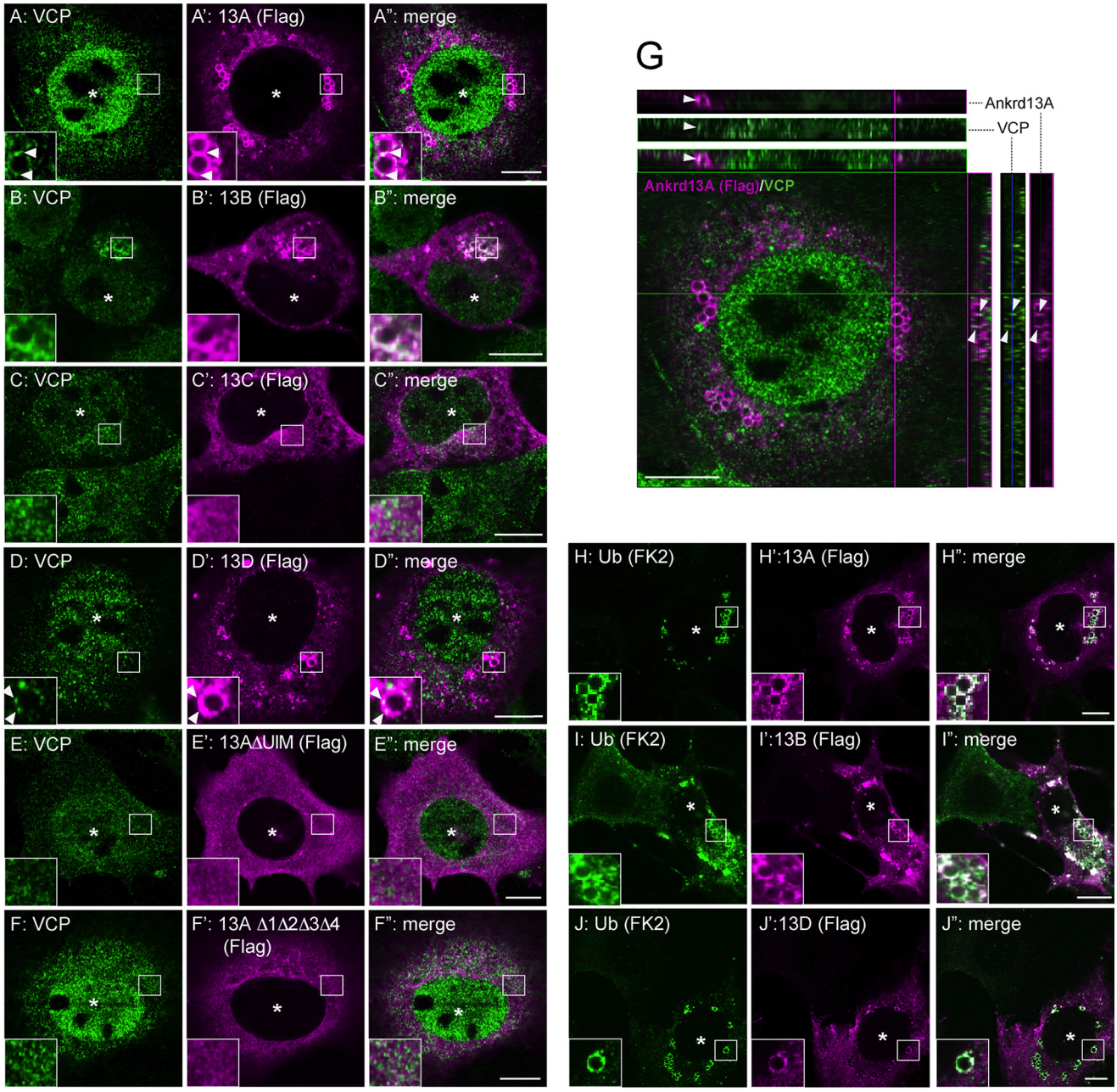

FIGURE 3. **Ankrd13 overexpression recruits VCP and Ub-protein conjugates to enlarged late endosomes.** *A–F"*, COS-7 cells were transfected with FLAG-Ankrd13 proteins or Ankrd13A mutants and double-stained with anti-VCP (*A–F*) and anti-FLAG (*A'–F'*) antibodies. *G*, a representative of the orthogonal reconstruction of 10 confocal slices of Ankrd13A-expressing cells is shown in the *y-z* and *x-z* axes. *H–J"*, COS-7 cells were transfected with FLAG-tagged Ankrd13 proteins and double-stained with anti-Ub (*FK2*, *H–J*) and anti-FLAG (*H'–J'*) antibodies. *Asterisks* indicate nuclei in FLAG-Ankrd13-expressing cells. *Arrowheads* in *A–A"*, *D–D"*, and *G* indicate the co-localization sites of Ankrd13 proteins with VCP. *Insets* show higher magnification images of the regions indicated by *squares*. *Scale bar* = 10 μm. All panels are representatives of three independent experiments.

Overexpression of Ankrd13 Proteins Enlarges the Late Endosome—To examine the subcellular site of the Ankrd13-VCP interaction, we expressed FLAG-tagged Ankrd13A-13D as well as the Ankrd13A mutants in COS-7 cells. Immunofluorescence staining showed that the overexpression of Ankrd13A, 13B, and 13D caused enlarged hollow spherical structures in the cytoplasm, in which they co-localized with the late endosomal protein cation-independent mannose 6-phosphate receptor (CI-M6PR), on the limiting membrane (Fig. 2*A–B"* and *D–D"*, *arrowheads*). The aberrant structure was negative for the early endosome protein EEA1 (data not shown). In contrast, Ankrd13C exhibited uniform cytoplasmic staining and did not cause the formation of enlarged endosomes (Fig. 2, *C–C"*). Although overexpression of Ankrd13AΔAR was capable of inducing enlarged endosomes (Fig. 2, *E–E"*), ΔUIM and Δ1Δ2Δ3Δ4 were not (Fig. 2, *F–G"*), indicating that overexpression of Ankrd13 proteins causes enlarged late endosomes in an UIM-dependent manner.

Overexpressed Ankrd13 Proteins Co-localize with VCP and Ub Protein Conjugates on the Late Endosome—We next examined the subcellular localization of VCP in Ankrd13-overexpressing cells. COS-7 cells were transfected with FLAG-tagged

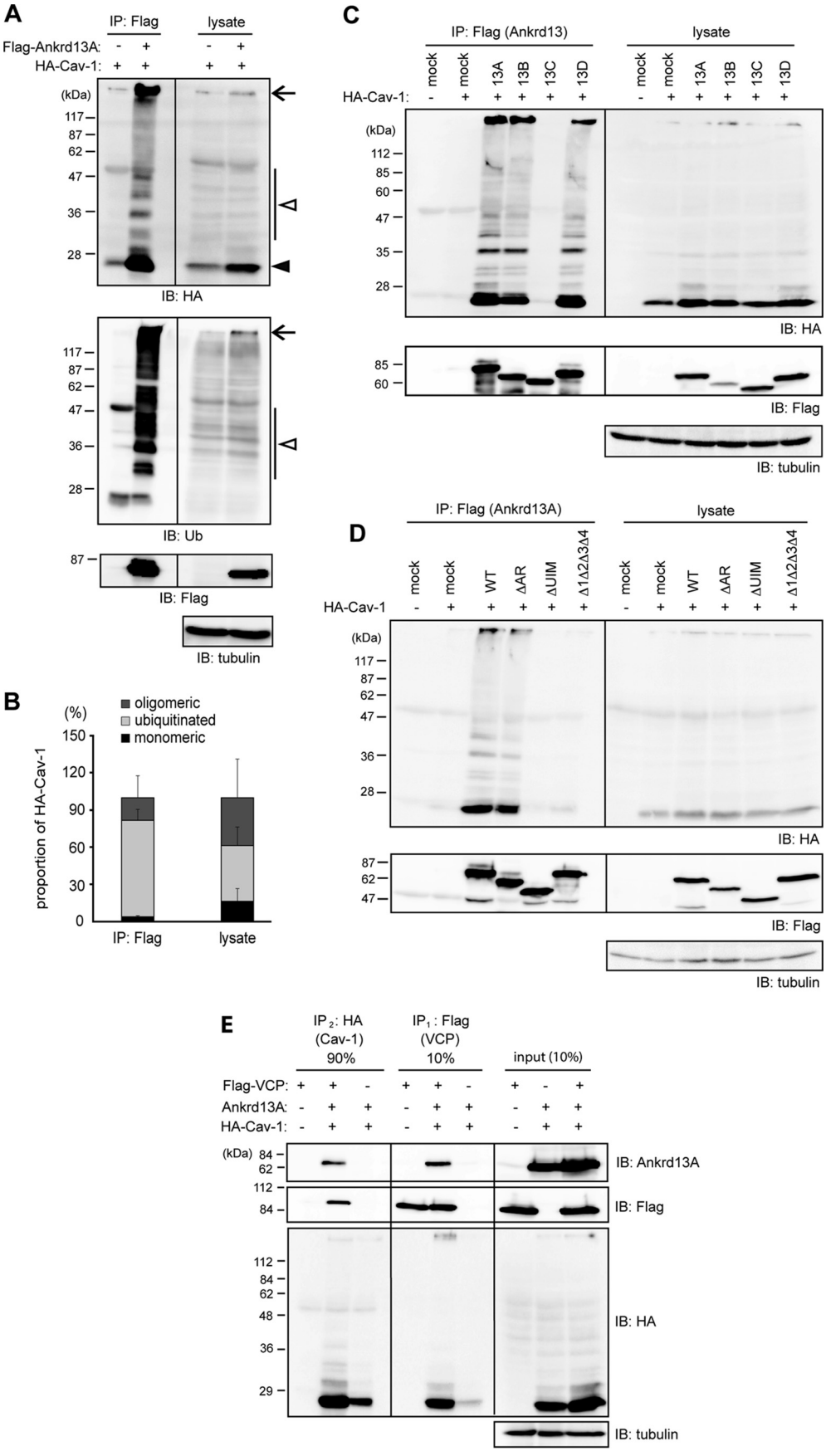
A
IP: Flag
lysate
Flag-Ankrd13A: - + - +
HA-Cav-1: + + + +
(kDa)
117
87
62
47
36
28
IB: HA
IB: Ub
IB: Flag
IB: tubulin
B
(%)
oligomeric
ubiquitinated
monomeric
proportion of HA-Cav-1
150
120
90
60
30
0
IP: Flag
lysate
C
IP: Flag (Ankrd13)
lysate
mock
13A
13B
13C
13D
HA-Cav-1: - + + + + +
112
85
60
47
35
28
IB: HA
IB: Flag
IB: tubulin
D
IP: Flag (Ankrd13A)
lysate
mock
WT
ΔAR
ΔUIM
Δ1Δ2Δ3Δ4
HA-Cav-1 - + + + + +
117
87
62
47
36
28
IB: HA
IB: Flag
IB: tubulin
E
IP2: HA (Cav-1) 90%
IP1: Flag (VCP) 10%
input (10%)
Flag-VCP: + + - + + - + - +
Ankrd13A: - + + - + + - + +
HA-Cav-1: - + + - + + - + +
(kDa)
84
62
112
84
48
36
29
IB: Ankrd13A
IB: Flag
IB: HA
IB: tubulin

Ankrd13A, 13B, or 13D and the Ankrd13A mutants and double-stained with anti-FLAG and anti-VCP antibodies. Endogenous VCP localized on the subdomains of the limiting membrane of the enlarged endosomes positive for Ankrd13A, 13B, or 13D (Fig. 3, *A–B"*, *D–D"*, and *G*, *arrowheads*), suggesting that Ankrd13 proteins interact with VCP on the endosome. Although the deletion of ankyrin repeats did not affect the effect of Ankrd13A on VCP localization (data not shown), ΔUIM and Δ1Δ2Δ3Δ4 did not co-localize with VCP (Fig. 3, *E–F"*), consistent with the requirement of UIMs for Ankrd13A binding to VCP (Fig. 1*E*).

Staining of Ankrd13-transfected cells with the anti-Ub antibody FK2, which specifically recognizes Ub-protein conjugates (23), showed that ubiquitinated proteins accumulated on the limiting membrane of enlarged endosomes, caused by the overexpression of Ankrd13A, 13B, or 13D (Fig. 3, *H–J"*). The accumulation of Ub-protein conjugates was not observed in cells expressing the ΔUIM or Δ1Δ2Δ3Δ4 mutant of Ankrd13A (data not shown).

Ankrd13 Proteins Bind to Cav-1—Endosomal VCP has been shown to facilitate the lysosomal trafficking of Cav-1 (12). Because Ankrd13 proteins co-localized with VCP on the endosome, we examined whether they also interact with Cav-1. Because of the slow turnover rate of endogenous Cav-1, which leads to difficulties when investigating its lysosomal trafficking and degradation, overexpressed Cav-1 is used to increase its trafficking rate and provide a platform for examining the endocytosis of Cav-1 (5). Therefore, we co-transfected COS-7 cells with FLAG-Ankrd13A and C-terminally HA-tagged Cav-1 and immunoprecipitated Ankrd13A from the cell lysate. Anti-HA immunoblotting revealed that Ankrd13A co-precipitated not only monomeric Cav-1 (Fig. 4*A*, *first panel*, *black arrowhead*) but also multiple higher molecular weight bands, most likely representing the mono- and polyubiquitinated forms of Cav-1 because they were also positive on anti-Ub immunoblots (Fig. 4*A*, *first* and *second panels*, *white arrowheads*). We observed another extremely high molecular weight band (Fig. 4*A*, *first* and *second panels*, *arrows*), which corresponded to the 70S oligomeric form of Cav-1 (12). Quantification of the intensities of bands for unmodified, ubiquitinated, and oligomeric Cav-1 in the lysate and in the anti-FLAG immunoprecipitate revealed that ubiquitinated and oligomeric Cav-1 interacted with Ankrd13A more efficiently than unmodified monomeric Cav-1 (Fig. 4*B*). Examination of the interaction of HA-Cav-1 with other FLAG-tagged Ankrd13 isoforms and mutants showed that Cav-1 is co-precipitated with Ankrd13B, 13D, or Ankrd13AΔAR but not with Ankrd13C or Ankrd13AΔUIM (Fig. 4, *C* and *D*), suggesting that the Ankrd13-Cav-1 interaction requires the UIMs of Ankrd13 proteins. These results implicate Ankrd13 proteins in the VCP-mediated regulation of endosomal Cav-1 trafficking.

Ankrd13, VCP, and Cav-1 Form a Ternary Complex—In an attempt to elucidate the functional relationship between Ankrd13, VCP, and Cav-1, we examined whether they are involved in the same complex in the cell. FLAG-VCP, HA-Cav-1, and untagged Ankrd13A were co-expressed in COS-7 cells. After cell lysis, VCP was immunoisolated with anti-FLAG antibody-immobilized beads and eluted from the beads with the FLAG peptide. Immunoblotting showed that HA-Cav-1 and Ankrd13A were both co-precipitated with FLAG-VCP, although nonspecific HA-Cav-1 precipitation was detected weakly in cells not expressing FLAG-VCP (Fig. 4*E*). The eluate was then subjected to a second immunoprecipitation with the anti-HA antibody, which revealed that Ankrd13A was co-isolated sequentially with VCP and then Cav-1 (Fig. 4*E*), suggesting that the three proteins form a ternary complex *in vivo*.

Cav-1 Is Conjugated with Lys-63-linked Ub Chains—Given that Ankrd13 proteins co-precipitated ubiquitinated Cav-1 (Fig. 4*A*) and that Ankrd13 UIMs bind preferentially to Lys-63-linked Ub chains *in vitro* (18), we determined the types of Ub chain modifications on Cav-1 using the absolute quantification strategy in combination with LC-MS/MS (Fig. 5*A*). COS-7 cells expressing FLAG-tagged Cav-1 were lysed in the presence of 1% SDS to dissociate Cav-1 from its associated proteins. After dilution with buffer containing 1% Triton X-100, FLAG-Cav-1 was immunoprecipitated and subjected to SDS-PAGE. The part of the gel containing unmodified and ubiquitinated Cav-1 was excised (Fig. 5*B*, *dashed lines*), trypsinized, and examined by LC-MS/MS. Successful immunoprecipitation of Cav-1 was confirmed by immunoblotting (Fig. 5*C*). We found that Cav-1 is decorated primarily with a Lys-63-linked Ub chain (Fig. 5*D*, *64%*). A Lys-48-linked chain was detected at 28% (Fig. 5*D*). In addition, the abundance of other atypical chain types, including Met-1-, Lys-6-, Lys-11-, Lys-27-, Lys-29-, and Lys-33-linked chains, fell below 5% (Fig. 5*D*). These results suggest that Cav-1 mainly undergoes Lys-63-linked polyubiquitination, which was consistent with its role in endocytosis.

Using the MS approach, we also determined the types of Ub chains to which Ankrd13 proteins bind in the cell (Fig. 5*A*). The FLAG-tagged Ankrd13A WT and Δ1Δ2Δ3Δ4 mutant were immunoprecipitated from transfected COS-7 cells. After SDS-PAGE of the precipitates, the gel region containing all of the loaded proteins was excised (Fig. 5*E*, *dashed lines*), trypsinized, and subjected to LC-MS/MS. Successful immunoprecipitation was verified by immunoblotting (Fig. 5*F*). Quantitative analyses showed that, in cells expressing WT Ankrd13A, substantial amounts of Lys-48- and Lys-63-linked Ub chains were co-precipitated (Fig. 5*G*, *left panel*, *49%* and *37%* for Lys-48- and Lys-

FIGURE 4. **Ankrd13 proteins bind to Cav-1.** *A*, lysates of COS-7 cells co-transfected with FLAG-Ankrd13A and HA-Cav-1 were immunoprecipitated (*IP*) with an anti-FLAG antibody and immunoblotted (*IB*) with the indicated antibodies. The *black arrowhead*, *white arrowheads*, and *arrows* indicate the unmodified monomeric, ubiquitinated, and oligomeric forms of Cav-1, respectively. *B*, quantification of the immunoblot data in *A*, demonstrating the proportion of unmodified monomeric, ubiquitinated, and oligomeric forms of Cav-1 in the Ankrd13A immunoprecipitate (*IP: FLAG*) and cell lysate. Data are normalized against mock-transfected cells and shown as the mean ± S.D. of three independent experiments. *C* and *D*, HA-Cav-1 was transfected into COS-7 cells together with FLAG-tagged Ankrd13 proteins (*C*) or Ankrd13A mutants (*D*) and examined by co-immunoprecipitation experiments as in *A*. The 8S and 70S Cav-1 oligomers were not separated by SDS-PAGE with a high concentration (12%) of acrylamide in *A*, *C*, and *D*. *E*, the lysate of COS-7 cells transfected with FLAG-VCP, HA-Cav-1, and untagged Ankrd13A was subjected to sequential immunoprecipitation. VCP was first immunoprecipitated with an anti-FLAG antibody (IP_1) and then eluted from the antibody with the FLAG peptide. The eluate was then immunoprecipitated with an anti-HA antibody (IP_2), and the IP_1 and IP_2 precipitates were immunoblotted with the indicated antibodies. The experiments in *C*, *D*, and *E* were repeated at least three times.

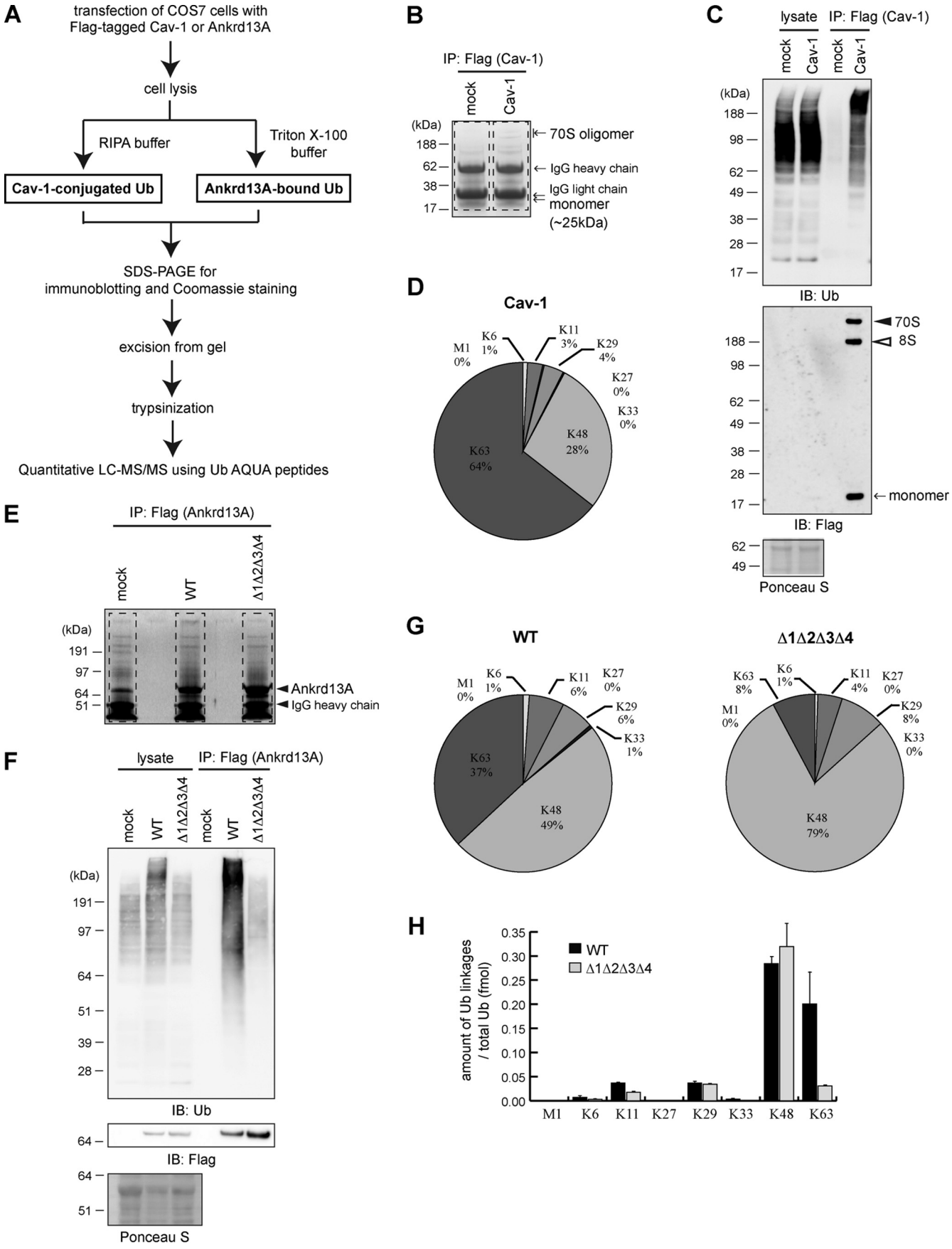
A
transfection of COS7 cells with Flag-tagged Cav-1 or Ankrd13A
cell lysis
RIPA buffer
Triton X-100 buffer
Cav-1-conjugated Ub
Ankrd13A-bound Ub
SDS-PAGE for immunoblotting and Coomassie staining
excision from gel
trypsinization
Quantitative LC-MS/MS using Ub AQUA peptides
B
IP: Flag (Cav-1)
mock
Cav-1
(kDa)
188
62
38
17
70S oligomer
IgG heavy chain
IgG light chain
monomer (~25kDa)
C
lysate
IP: Flag (Cav-1)
mock
Cav-1
mock
Cav-1
(kDa)
188
98
62
49
38
28
17
IB: Ub
70S
8S
monomer
IB: Flag
62
49
Ponceau S
D
Cav-1
M1 0%
K6 1%
K11 3%
K29 4%
K27 0%
K33 0%
K48 28%
K63 64%
E
IP: Flag (Ankrd13A)
mock
WT
Δ1Δ2Δ3Δ4
(kDa)
191
97
64
51
Ankrd13A
IgG heavy chain
F
lysate
IP: Flag (Ankrd13A)
mock
WT
Δ1Δ2Δ3Δ4
mock
WT
Δ1Δ2Δ3Δ4
(kDa)
191
97
64
51
39
28
IB: Ub
64
IB: Flag
64
51
Ponceau S
G
WT
M1 0%
K6 1%
K11 6%
K27 0%
K29 6%
K33 1%
K63 37%
K48 49%
Δ1Δ2Δ3Δ4
K63 8%
K6 1%
K11 4%
K27 0%
M1 0%
K29 8%
K33 0%
K48 79%
H
amount of Ub linkages / total Ub (fmol)
0.35
0.30
0.25
0.20
0.15
0.10
0.05
0.00
WT
Δ1Δ2Δ3Δ4
M1
K6
K11
K27
K29
K33
K48
K63

63-linked chains, respectively). Other chain types were detected at low levels of less than 10% (Fig. 5*G*, *left panel*). By contrast, in the Δ1Δ2Δ3Δ4 mutant, the proportion of co-precipitated Lys-63-linked Ub chains decreased significantly to 8% (Fig. 5*G*, *right panel*). Calculation of the level of each Ub chain type against the total Ub level revealed that, although the levels of Lys-48-linked Ub chains were similar between the co-precipitates of the WT and Δ1Δ2Δ3Δ4 mutant of Ankrd13A, that of Lys-63-linked chains decreased significantly when the UIMs were mutated (Fig. 5*H*). These results support our previous finding that the UIM domains of Ankrd13A bind preferentially to the Lys-63-linked Ub chain.

Cav-1 Co-localizes with Overexpressed Ankrd13 Proteins on the Late Endosome—We examined the co-localization of Ankrd13 proteins and Cav-1 in the cell. COS-7 cells were co-transfected with HA-Cav-1 and FLAG-Ankrd13 proteins. Immunostaining of the fixed cells with anti-HA and anti-FLAG antibodies revealed that, although Cav-1 was localized to cytoplasmic punctate structures in the absence of Ankrd13 transfection (Fig. 6, *A–A″*), it co-localized with overexpressed Ankrd13A, 13B, and 13D, but not 13C, on the limiting membrane of the enlarged endosomes (Fig. 6, *B–E″*). Cav-1 also co-localized with ΔAR but not the ΔUIM or Δ1Δ2Δ3Δ4 mutant of Ankrd13A, suggesting that overexpression of Ankrd13 proteins causes the endosomal accumulation of Cav-1 in an UIM-dependent manner (Fig. 6, *F–H″*).

Overexpression of Ankrd13 Proteins Stabilizes the Ubiquitinated Cav-1 Oligomer—To elucidate the endosomal function of Ankrd13 proteins, we hypothesized that they play a role with VCP in regulating the oligomeric state of Cav-1. We co-transfected HA-Cav-1 and FLAG-Ankrd13 proteins into COS-7 cells and examined the amount of the Cav-1 oligomers in the lysate. Cell lysates were suspended in low-SDS sample buffer and subjected to SDS-PAGE without prior boiling to retain the oligomeric state of Cav-1 during sample preparation (see "Experimental Procedures" for details) (12). Blotting with the anti-HA antibody showed that the overexpression of Ankrd13A and its ΔAR mutant led to the accumulation of Cav-1 70S oligomer (Fig. 7*A*). The difference observed in Cav-1 oligomer levels between the WT and the ΔAR mutant could be due to differences in their expression levels (Fig. 7*A*, *center panel*). This effect was dependent on UIMs because the two UIM mutants of Ankrd13A lost this ability (Fig. 7*A*). To confirm that this effect is specific to Ankrd13 proteins, we examined the effect of the overexpression of STAM1, an UIM-bearing ESCRT-0 component that sorts ubiquitinated cargo on the endosome (21), and found that the stabilizing effect of STAM1 on the Cav-1 oligomer was significantly less than that of Ankrd13A (Fig. 7*B*).

The ubiquitination of Cav-1 at the N-terminal region is necessary for its VCP interaction and lysosomal trafficking (5, 24). Therefore, we substituted the six Lys residues (Lys-5, Lys-26, Lys-30, Lys-39, Lys-47, and Lys-57) in the N-terminal region of Cav-1 with Arg (Fig. 7*C*, *K5–57R*). The 70S oligomer of this mutant was not stabilized by overexpression of Ankrd13A, suggesting that Ankrd13 proteins participate in the oligomer stabilization of ubiquitinated Cav-1 (Fig. 7*D*).

Interaction with Ankrd13A Is Compromised in IBMPFD-associated VCP Mutants—Missense mutations in the *VCP* gene have been identified as the cause of neurodegenerative diseases, including IBMPFD (25, 26). Fibroblasts from patients with IBMPFD accumulate Cav-1 on the limiting membrane of the enlarged late endosome (12). Because the effects of Ankrd13 overexpression shown in Fig. 2 were reminiscent of this phenotype, we examined the interaction between Ankrd13A and the IBMPFD-associated VCP mutants R95G, R155H, and A232E. As a control, the E578Q mutant, capable of substrate binding but not ATP hydrolysis (25, 27), was used. FLAG-tagged WT and the mutants of VCP were expressed in COS-7 cells, and their lysates were examined by anti-FLAG immunoprecipitation, followed by immunoblotting with the anti-Ankrd13A antibody. Although WT and the E578Q mutant of VCP successfully co-precipitated Ankrd13A, the activity of the three disease-related mutants was reduced significantly (Fig. 7*E*). Consistent with previous findings (12), the interaction between the disease-related VCP mutants and Cav-1 was also diminished (data not shown). These results further support mutations in *VCP* in patients with IBMPFD being relevant to the compromised endocytic trafficking of Cav-1.

Discussion

Ankrd13 Forms a Ternary Complex with VCP and Cav-1 on the Endosome—In this study, we showed that Ankrd13A is involved in the same protein complex with VCP and Cav-1 (Fig. 4). This complex was expected to occur *in vivo* because the interaction between endogenous Ankrd13 and VCP was also detected (Fig. 1). The requirement for ubiquitination and the UIMs in Ankrd13 proteins in this interaction (Fig. 1) was consistent with the Ub-dependent function of VCP (13, 14).

Because VCP and Cav-1 accumulated on the limiting membrane of the CI-M6PR-positive endosome in Ankrd13-overexpressing cells, the ternary complex was likely to be localized on the late endosome (Figs. 3 and 6). In co-immunoprecipitation experiments, the interaction between Ankrd13 proteins and VCP was only detected when cell lysates were prepared in the presence of NEM, an inhibitor of cysteine proteases to which most deubiquitinases belong (Fig. 1). Furthermore, this interaction was abolished when the UIMs of Ankrd13A, particularly

FIGURE 5. **Identification of Ub chain types conjugated to Cav-1 and bound to Ankrd13A.** *A*, the procedures of sample preparation for the LC-MS/MS of Cav1-conjugated and Ankrd13A-bound Ub chains. *RIPA*, radio-immunoprecipitation assay; *AQUA*, absolute quantification. *B*, the lysates of COS-7 cells transfected with FLAG-Cav-1 were subjected to anti-FLAG immunoprecipitation (*IP*) followed by SDS-PAGE and Coomassie staining. The regions enclosed by *dashed lines* were excised and analyzed by LC-MS/MS. *C*, aliquots of the immunoprecipitates in *B* were immunoblotted (*IB*) with the indicated antibodies. *D*, the percentages of Ub chain types in immunoprecipitated FLAG-Cav-1 in *B* analyzed by LC-MS/MS. *E* and *F*, the lysates of COS-7 cells transfected with FLAG-tagged WT Ankrd13A or the Δ1Δ2Δ3Δ4 mutant were subjected to anti-FLAG immunoprecipitation followed by Coomassie staining (*E*) and immunoblotting (*F*). The regions enclosed by *dashed lines* in *E* were excised and analyzed by LC-MS/MS. *G*, the percentages of Ub chain types bound to WT Ankrd13A (*left panel*) and Δ1Δ2Δ3Δ4 (*right panel*). All data represent the average values obtained from three independent experiments. *H*, the absolute amounts of Ub chain types bound to Ankrd13A WT and Δ1Δ2Δ3Δ4 mutant prepared in *E* and *F*. *Error bars* indicate mean ± S.D.

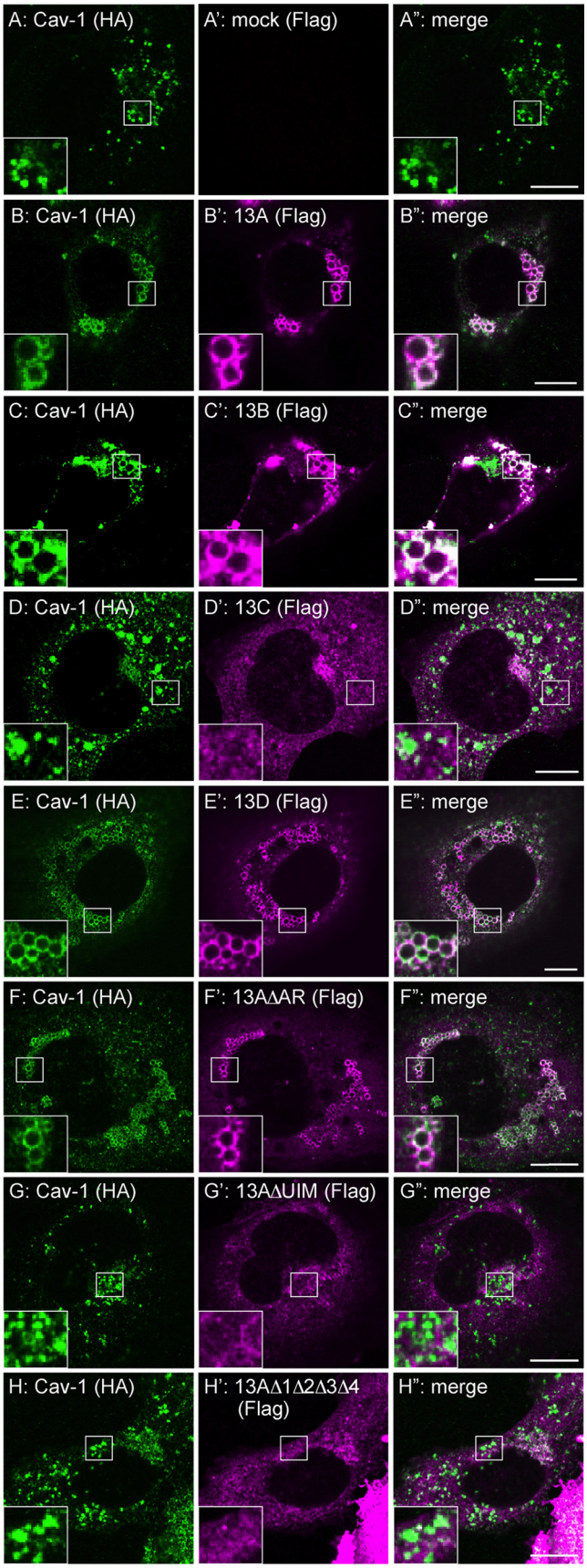

FIGURE 6. **Ankrd13 overexpression recruits Cav-1 to enlarged late endosomes.** COS-7 cells were transfected with HA-Cav-1 together with FLAG-tagged Ankrd13 proteins or Ankrd13A mutants and double-stained with anti-HA (*A–H*) and anti-FLAG (*A′–H′*) antibodies. *Insets* show higher magnification images of the regions indicated by *squares*. *Scale bars* = 10 μm. All panels are representatives of three independent experiments.

UIM3 and UIM4, which are critical for Ub binding (18), were functionally mutated. The interaction was shown to be indirect because purified Ankrd13A and VCP failed to bind to each other (Fig. 1). These results suggest that the interaction between Ankrd13 proteins and VCP is mediated by ubiquitinated proteins. Cav-1 is a likely candidate for such a ubiquitinated adaptor because Ankrd13A UIMs preferentially bind to the Lys-63-linked Ub chain (Fig. 5) (18), and we showed here, for the first time, that Cav-1 mainly undergoes Lys-63-linked polyubiquitination (Fig. 5). Because the interaction between VCP and Cav-1 also depends on Cav-1 ubiquitination (12), our findings implicate Ankrd13 proteins in regulating the VCP-dependent lysosomal trafficking of Cav-1 modified with the Lys-63-linked Ub chain.

Ankrd13 Participates in Lysosomal Trafficking of Cav-1—VCP has been shown to bind to ubiquitinated Cav-1, facilitating the trafficking of Cav-1 to the lysosome (12). VCP binds with higher affinity to Cav-1 oligomers than to its monomer, raising the possibility that VCP promotes Cav-1 trafficking by segregating the Cav-1 70S oligomers to monomers on the MVB (12). In this study, we showed that the overexpression of Ankrd13 proteins increased Cav-1 70S oligomer levels in an UIM-dependent manner (Fig. 7). This effect was abolished when Cav-1 was mutated at the six N-terminally located Lys residues that undergo ubiquitination (Fig. 7). Together with the accumulation of Cav-1 on the endosome in Ankrd13-overexpressing cells (Fig. 6), these results suggest that Ankrd13 proteins participate in the ubiquitination-dependent endocytic trafficking of Cav-1. Consistently, the binding affinity of Ankrd13 proteins was higher for ubiquitinated and oligomerized Cav-1 than for unmodified monomeric Cav-1 (Fig. 4). In addition, the effect of stabilizing Cav-1 oligomers was specific to Ankrd13 proteins because the overexpression of STAM1, a UIM-bearing component of ESCRT-0, did not exhibit this effect (Fig. 7). Therefore, the stabilization of Cav-1 oligomers by Ankrd13 proteins is unlikely to be an artificial effect of overexpressing Ub-binding endosomal proteins. On the other hand, we have reported previously that, although overexpression of Ankrd13 proteins inhibits rapid endocytosis of EGF-activated EGF receptor from the plasma membrane, it does not affect its degradation rate or lead to its endosomal accumulation (18). These results suggest a specific endosomal role for Ankrd13 proteins toward Cav-1.

The Role Of Ankrd13 In Lysosomal Trafficking of Cav-1—The mechanisms by which Ankrd13 proteins regulate lysosomal trafficking of Cav-1 currently remain unclear. Because VCP mediates the disassembly or segregation of ubiquitinated protein complexes in various cellular events (13, 14), Ankrd13 proteins may cooperate with VCP to segregate Cav-1 70S oligomers (Fig. 8*B*). We have demonstrated previously that overexpressed Ankrd13 proteins localize to cytosolic punctate structures that are positive for endosomal proteins (18). Using higher-resolution fluorescence microscopy, we found in this study that overexpression of Ankrd13 proteins results in enlarged hollow endosomes, the limiting membrane of which

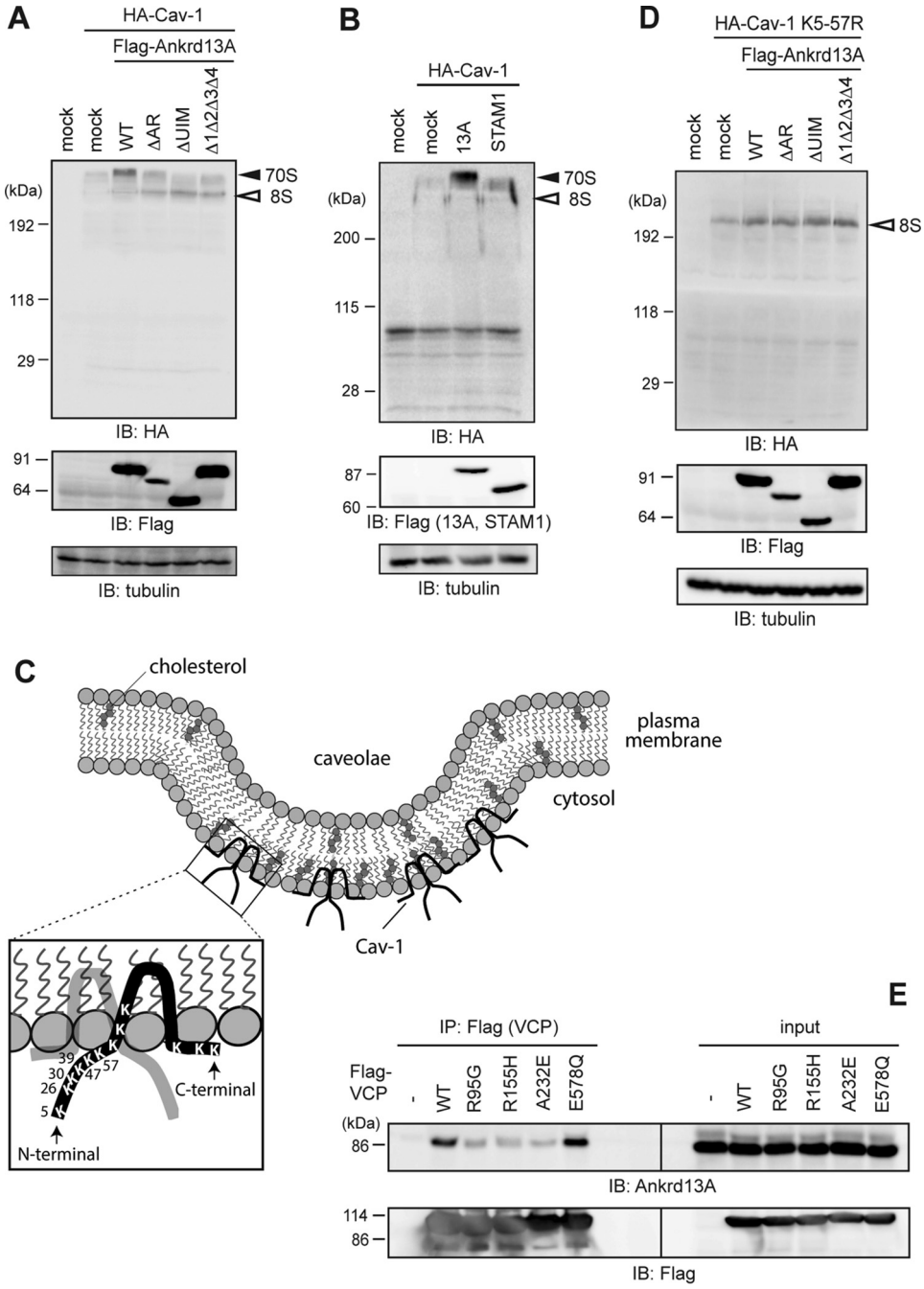

FIGURE 7. **Ankrd13A overexpression stabilizes the Cav-1 70S oligomer.** *A* and *B*, COS-7 cells were transfected with HA-Cav-1 together with FLAG-tagged Ankrd13A or its mutants (*A*) or FLAG-STAM1 (*B*). Cell lysates were prepared in low-SDS sample buffer without boiling. The same amounts of total proteins were immunoblotted with the indicated antibodies. *IB*, immunoblotting. *C*, schematics of the caveolae and human Cav-1, showing the positions of all Lys residues in Cav-1. Six Lys residues in the N-terminal region (Lys-5 to Lys-57) were replaced by Arg in the K5–57R mutant. *D*, COS-7 cells were transfected with HA-Cav-1 K5–57R together with FLAG-tagged Ankrd13A or its mutants. Cells were examined as in *A*. *E*, COS-7 cells were transfected with FLAG-tagged WT VCP or its mutants identified in patients with IBMPFD (*R95G*, *R155H*, and *A232E*) or lacking ATPase activity (*E578Q*). Their lysates were immunoprecipitated (*IP*) with an anti-FLAG antibody, and the precipitates were immunoblotted with the indicated antibodies. All the experiments were performed three times.

was positive for a late endosome marker (CI-M6PR) and Ub-protein conjugates (Figs. 2 and 3). Therefore, enlargement of the endosome may be caused by the impaired formation of MVB inner vesicles (*i.e.* invagination of the Cav-1 oligomer-containing limiting membrane into the lumen of the endosome), which, in turn, is due to the inhibition of Cav-1 oligomer segregation by Ankrd13 overexpression (Fig. 8*A*). Studies on the effects of depleting the endogenous Ankrd13 function on Cav-1 trafficking and endosomal morphology are important for assessing this possibility. However, the three Ankrd13 proteins (*i.e.* 13A, 13B, and 13D) are most likely to have redundant cellular functions (Ref. 18 and this study), and we have not yet successfully depleted these proteins simultaneously using RNA interference. Although the Ankrd13 family comprises three members in vertebrate species, a single *Ankrd13* gene is present in *Drosophila melanogaster* and *Caenorhabditis elegans*. It is therefore of interest to examine the effect of knocking down the single Ankrd13 protein in these animals.

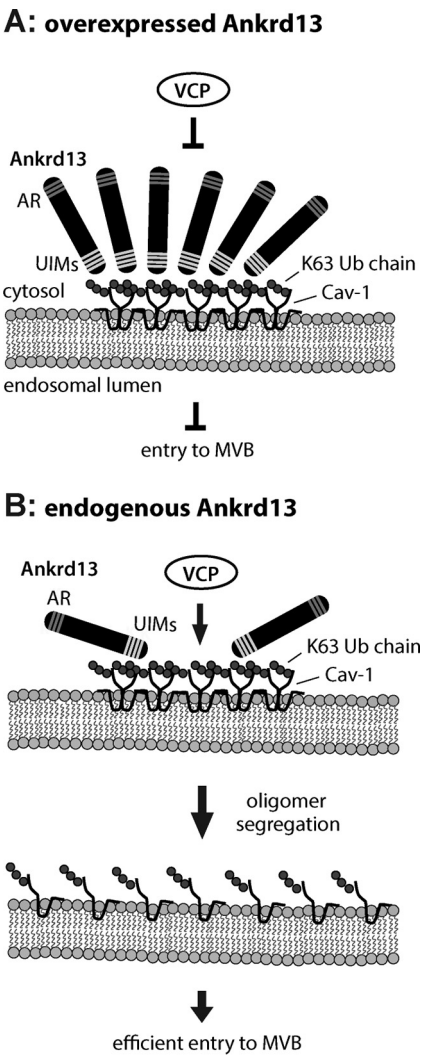

FIGURE 8. **Schematics for the Ankrd13 function on endosomal Cav-1 trafficking.** *A*, when overexpressed, Ankrd13 blocks VCP interaction with the Cav-1 oligomer on the endosomal membrane, inhibiting Cav-1 entry into inner vesicles of the MVB. *AR*, ankyrin repeat. *B*, endogenous Ankrd13 concentrates ubiquitinated Cav-1 on the endosomal membrane, facilitating VCP-mediated segregation of the Cav-1 oligomer and subsequent entry of Cav-1 into the MVB inner vesicles.

Although the N-terminal domain of VCP is capable of binding to ubiquitinated substrates, its affinity is weak, and its co-factors, which serve as adaptors for ubiquitinated substrates, are typically required for more efficient and specific substrate interactions (28, 29). Ubiquitin regulatory X (UBX) domain-containing proteins are the most popular co-factor family of VCP (30). They contain the VCP-binding UBX domain, and some harbor Ub-binding domains such as the ubiquitin-associated (UBA) domain, which binds to ubiquitinated substrates. The UBX domain protein UBXD-1 has been identified as a VCP co-factor in the endocytic trafficking of Cav-1 (12, 24). However, no Ub-binding site has been identified in UBXD1 (14, 31). Therefore, the mechanisms by which the VCP-UBXD1 complex recognizes ubiquitinated Cav-1 on the endosome remain unclear. Ankrd13 proteins may concentrate ubiquitinated Cav-1 on the endosomal membrane to facilitate lysosomal Cav-1 trafficking mediated by VCP and UBXD1.

The stabilization of ubiquitinated Cav-1 oligomers because of the overexpression of Ankrd13A (Fig. 7) could be due to an excess of Ankrd13 proteins binding to ubiquitinated Cav-1 on the endosome, thereby blocking binding of VCP to Cav-1 and preventing VCP-mediated segregation of Cav-1 oligomers (Fig. 8*A*). We hypothesize that, in normal cells, endogenous Ankrd13 proteins concentrate ubiquitinated Cav-1 oligomers to facilitate their interaction with VCP, leading to their segregation to Cav-1 monomers (Fig. 8*B*).

The molecular mechanisms underlying the ubiquitination-dependent lysosomal targeting of cell surface proteins have been examined intensively for monomeric or dimeric cargo. However, oligomerized membrane proteins may require additional mechanisms for efficient down-regulation because the incorporation of the large oligomers of cargo proteins into the inner vesicles of the MVBs may be less efficient and their prior segregation to monomers required. The function of VCP and Ankrd13 may not be restricted to Cav; they may play a more general role in the down-regulation of different kinds of oligomerized membrane proteins. Because the ortholog of Ankrd13 proteins in multicellular organisms is not found in yeast, this regulatory mechanism is expected to be acquired in metazoan cells.

Ankrd13 and IBMPFD—Previous studies have demonstrated that the VCP mutants identified in patients with IBMPFD induce the formation of enlarged empty late endosomes lacking intraluminal vesicles in transfected U2OS cells as well as in fibroblasts isolated from these patients (12). Inhibition of VCP activity by the chemical inhibitor *N2,N4*-dibenzylquinazoline-2,4-diamine or RNA interference-mediated depletion of its endosomal co-factor UBXD-1 also leads to the formation of enlarged hollow endosomes in WT cells (12). This endosomal morphology is reminiscent of that of the aberrant endosomes caused by Ankrd13 overexpression (Fig. 2). Furthermore, the IBMPFD-associated VCP mutants, which lack Cav-1-binding ability (12), also did not bind to Ankrd13 proteins (Fig. 7). These results further support the hypothesis that Ankrd13 proteins cooperate with VCP in the regulation of the endosome-to-lysosome trafficking of Cav-1 and suggest that disruption of the ternary complex by VCP, Cav-1, and Ankrd13 leads to a disease condition in human cells. Further studies on the precise role of Ankrd13 proteins in this process will not only be crucial for obtaining a better understanding of the mechanisms underlying the endocytic trafficking of oligomerized proteins but also be beneficial in the treatment of IBMPFD.

Author Contributions—D. B., Y. S., and M. K. conceived and coordinated the experiments. D. B. performed most of the experiments. H. Y., H. T., A. Y., and K. T. also performed experiments. D. B. and M. K. wrote the manuscript. All authors reviewed the results and approved the final version of the manuscript.

Acknowledgments—We thank Masami Nagahama and Eiki Kominami for reagents and Toshiaki Fukushima and Hikaru Tsuchiya for discussions.

References

1. Parton, R. G., and Simons, K. (2007) The multiple faces of caveolae. *Nat. Rev. Mol. Cell Biol.* **8,** 185–194

2. Hayer, A., Stoeber, M., Bissig, C., and Helenius, A. (2010) Biogenesis of caveolae: stepwise assembly of large caveolin and cavin complexes. *Traffic* **11,** 361–382
3. Parton, R. G., and del Pozo, M. A. (2013) Caveolae as plasma membrane sensors, protectors and organizers. *Nat. Rev. Mol. Cell Biol.* **14,** 98–112
4. Hill, M. M., Bastiani, M., Luetterforst, R., Kirkham, M., Kirkham, A., Nixon, S. J., Walser, P., Abankwa, D., Oorschot, V. M., Martin, S., Hancock, J. F., and Parton, R. G. (2008) PTRF-Cavin, a conserved cytoplasmic protein required for caveola formation and function. *Cell* **132,** 113–124
5. Hayer, A., Stoeber, M., Ritz, D., Engel, S., Meyer, H. H., and Helenius, A. (2010) Caveolin-1 is ubiquitinated and targeted to intralumenal vesicles in endolysosomes for degradation. *J. Cell Biol.* **191,** 615–629
6. Komander, D., and Rape, M. (2012) The ubiquitin code. *Annu. Rev. Biochem.* **81,** 203–229
7. Meierhofer, D., Wang, X., Huang, L., and Kaiser, P. (2008) Quantitative analysis of global ubiquitination in HeLa cells by mass spectrometry. *J. Proteome Res.* **7,** 4566–4576
8. Kaiser, S. E., Riley, B. E., Shaler, T. A., Trevino, R. S., Becker, C. H., Schulman, H., and Kopito, R. R. (2011) Protein standard absolute quantification (PSAQ) method for the measurement of cellular ubiquitin pools. *Nat. Methods* **8,** 691–696
9. Haglund, K., and Dikic, I. (2012) The role of ubiquitylation in receptor endocytosis and endosomal sorting. *J. Cell Sci.* **125,** 265–275
10. Tanno, H., and Komada, M. (2013) The ubiquitin code and its decoding machinery in the endocytic pathway. *J. Biochem.* **153,** 497–504
11. Saksena, S., Sun, J., Chu, T., and Emr, S. D. (2007) ESCRTing proteins in the endocytic pathway. *Trends Biochem. Sci.* **32,** 561–573
12. Ritz, D., Vuk, M., Kirchner, P., Bug, M., Schütz, S., Hayer, A., Bremer, S., Lusk, C., Baloh, R. H., Lee, H., Glatter, T., Gstaiger, M., Aebersold, R., Weihl, C. C., and Meyer, H. (2011) Endolysosomal sorting of ubiquitylated caveolin-1 is regulated by VCP and UBXD1 and impaired by VCP disease mutations. *Nat. Cell Biol.* **13,** 1116–1123
13. Jentsch, S., and Rumpf, S. (2007) Cdc48 (p97): a "molecular gearbox" in the ubiquitin pathway? *Trends Biochem. Sci.* **32,** 6–11
14. Meyer, H., Bug, M., and Bremer, S. (2012) Emerging functions of the VCP/p97 AAA-ATPase in the ubiquitin system. *Nat. Cell Biol.* **14,** 117–123
15. Wolf, D. H., and Stolz, A. (2012) The Cdc48 machine in endoplasmic reticulum associated protein degradation. *Biochim. Biophys. Acta* **1823,** 117–124
16. Johnson, J. O., Mandrioli, J., Benatar, M., Abramzon, Y., Van Deerlin, V. M., Trojanowski, J. Q., Gibbs, J. R., Brunetti, M., Gronka, S., Wuu, J., Ding, J., McCluskey, L., Martinez-Lage, M., Falcone, D., Hernandez, D. G., Arepalli, S., Chong, S., Schymick, J. C., Rothstein, J., Landi, F., Wang, Y. D., Calvo, A., Mora, G., Sabatelli, M., Monsurrò, M. R., Battistini, S., Salvi, F., Spataro, R., Sola, P., Borghero, G.; ITALSGEN Consortium, Galassi, G., Scholz, S. W., Taylor, J. P., Restagno, G., Chiò, A., and Traynor, B. J. (2010) Exome sequencing reveals VCP mutations as a cause of familial ALS. *Neuron* **68,** 857–864
17. Spina, S., Van Laar, A. D., Murrell, J. R., Hamilton, R. L., Kofler, J. K., Epperson, F., Farlow, M. R., Lopez, O. L., Quinlan, J., DeKosky, S. T., and Ghetti, B. (2013) Phenotypic variability in three families with valosin-containing protein mutation. *Eur. J. Neurol.* **20,** 251–258
18. Tanno, H., Yamaguchi, T., Goto, E., Ishido, S., and Komada, M. (2012) The Ankrd 13 family of UIM-bearing proteins regulates EGF receptor endocytosis from the plasma membrane. *Mol. Biol. Cell* **23,** 1343–1353
19. Kato, M., Miyazawa, K., and Kitamura, N. (2000) A deubiquitinating enzyme UBPY interacts with the Src homology 3 domain of Hrs-binding protein via a novel binding motif P*X*(V/I)(D/N)R*XX*KP. *J. Biol. Chem.* **275,** 37481–37487
20. Nagahama, M., Ohnishi, M., Kawate, Y., Matsui, T., Miyake, H., Yuasa, K., Tani, K., Tagaya, M., and Tsuji, A. (2009) UBXD1 is a VCP-interacting protein that is involved in ER-associated degradation. *Biochem. Biophys. Res. Commun.* **382,** 303–308
21. Mizuno, E., Kawahata, K., Kato, M., Kitamura, N., and Komada, M. (2003) STAM proteins bind ubiquitinated proteins on the early endosome via the VHS domain and ubiquitin-interacting motif. *Mol. Biol. Cell* **14,** 3675–3689
22. Tsuchiya, H., Tanaka, K., and Saeki, Y. (2013) The parallel reaction monitoring method contributes to a highly sensitive polyubiquitin chain quantification. *Biochem. Biophys. Res. Commun.* **436,** 223–229
23. Fujimuro, M., and Yokosawa, H. (2005) Production of antipolyubiquitin monoclonal antibodies and their use for characterization and isolation of polyubiquitinated proteins. *Methods Enzymol.* **399,** 75–86
24. Kirchner, P., Bug, M., and Meyer, H. (2013) Ubiquitination of the N-terminal region of caveolin-1 regulates endosomal sorting by the VCP/p97 AAA-ATPase. *J. Biol. Chem.* **288,** 7363–7372
25. Watts, G. D., Wymer, J., Kovach, M. J., Mehta, S. G., Mumm, S., Darvish, D., Pestronk, A., Whyte, M. P., and Kimonis, V. E. (2004) Inclusion body myopathy associated with Paget disease of bone and frontotemporal dementia is caused by mutant valosin-containing protein. *Nat. Genet.* **36,** 377–381
26. Tang, W. K., and Xia, D. (2013) Altered intersubunit communication is the molecular basis for functional defects of pathogenic p97 mutants. *J. Biol. Chem.* **288,** 36624–36635
27. Ramadan, K., Bruderer, R., Spiga, F. M., Popp, O., Baur, T., Gotta, M., and Meyer, H. H. (2007) Cdc48/p97 promotes reformation of the nucleus by extracting the kinase Aurora B from chromatin. *Nature* **450,** 1258–1262
28. Dai, R. M., and Li, C. C. (2001) Valosin-containing protein is a multi-ubiquitin chain-targeting factor required in ubiquitin-proteasome degradation. *Nat. Cell Biol.* **3,** 740–744
29. Meyer, H. H., Wang, Y., and Warren, G. (2002) Direct binding of ubiquitin conjugates by the mammalian p97 adaptor complexes, p47 and Ufd1-Npl4. *EMBO J.* **21,** 5645–5652
30. Schuberth, C., and Buchberger, A. (2008) UBX domain proteins: major regulators of the AAA ATPase Cdc48/p97. *Cell Mol. Life Sci.* **65,** 2360–2371
31. Alexandru, G., Graumann, J., Smith, G. T., Kolawa, N. J., Fang, R., and Deshaies R. J. (2008) UBXD7 binds multiple ubiquitin ligases and implicates p97 in HIF1α turnover. *Cell* **134,** 804–816